Quantum Squeezing and Sensing with Pseudo-Anti-Parity-Time Symmetry

Xi-Wang Luo, Chuanwei Zhang, and Shengwang Du

Phys. Rev. Lett. **128**, 173602 — Published 29 April 2022

DOI: 10.1103/PhysRevLett.128.173602

Quantum squeezing and sensing with pseudo anti-parity-time symmetry

Xi-Wang Luo,[1] Chuanwei Zhang,[1,*] and Shengwang Du[1,†]

[1] *Department of Physics, The University of Texas at Dallas, Richardson, Texas 75080-3021, USA*

The emergence of parity-time ($\mathcal{PT}$) symmetry has greatly enriched our study of symmetry-enabled non-Hermitian physics, but the realization of quantum $\mathcal{PT}$-symmetry faces an intrinsic issue of unavoidable symmetry-breaking Langevin noises. Here we construct a quantum pseudo-anti-$\mathcal{PT}$ (pseudo-$\mathcal{APT}$) symmetry in a two-mode bosonic system without involving Langevin noises. We show that the spontaneous pseudo-$\mathcal{APT}$ symmetry breaking leads to an exceptional point, across which there is a transition between different types of quantum squeezing dynamics, *i.e.*, the squeezing factor increases exponentially (oscillates periodically) with time in the pseudo-$\mathcal{APT}$ symmetric (broken) region. Such dramatic changes of squeezing factors and quantum dynamics near the exceptional point are utilized for ultra-precision quantum sensing. These exotic quantum phenomena and sensing applications can be experimentally observed in two physical systems: spontaneous wave mixing nonlinear optics and atomic Bose-Einstein condensates. Our work offers a physical platform for investigating exciting $\mathcal{APT}$ symmetry physics in the quantum realm, paving the way for exploring fundamental quantum non-Hermitian effects and their quantum technological applications.

Introduction.—Hermiticity and real eigenvalues of a Hamiltonian are key postulates of quantum mechanics. While non-Hermitian Hamiltonians emerged from the interaction with external environments generally possess complex eigenspectra, they can exhibit entirely real eigenvalues in the presence of parity-time ($\mathcal{PT}$) symmetry [1–7]. When the non-Hermiticity parameter exceeds a critical value, known as exceptional point (EP), the $\mathcal{PT}$-symmetry can be spontaneously broken for the eigenstates, leading to a phase transition from the $\mathcal{PT}$-symmetric phase with purely real eigenvalues to the $\mathcal{PT}$-broken phase with complex conjugate eigenvalue pairs. In the past decade, significant experimental and theoretical progress [8–20] has been made for exploring $\mathcal{PT}$-symmetry physics in various physical systems (e.g., photonics, acoustics, ultracold atoms, etc.), which generally utilize the control of linear gain/loss in classical wave systems. However, an intrinsic issue for studying $\mathcal{PT}$-symmetry physics in the quantum realm [21–27] is that a $\mathcal{PT}$-symmetric Hamiltonian involving linear gain/loss does not preserve the commutation relations of quantum field operators, therefore Langevin noises, which break $\mathcal{PT}$ symmetry, must be included in quantum systems [28]. Two experimental approaches to circumvent this issue for quantum $\mathcal{PT}$-symmetry include discarding quantum noise through post-selection measurement [25] and Hamiltonian dilation by embedding a non-Hermitian Hamiltonian into a larger Hermitian system [26].

Anti-$\mathcal{PT}$ ($\mathcal{APT}$) represents another non-Hermitian symmetry with the Hamiltonian *anticommuting* with $\mathcal{PT}$ operator (*i.e.*, $\{H_{APT}, \mathcal{PT}\} = 0$ instead of commutation $[H_{PT}, \mathcal{PT}] = 0$ for $\mathcal{PT}$-symmetry) and has recently attracted great interests [29–38]. Similar as $\mathcal{PT}$ symmetry, the spontaneous breaking of $\mathcal{APT}$ symmetry also leads to the emergence of EPs. Recent studies showed that an $\mathcal{APT}$-symmetric system does not have to involve linear gain/loss of classical fields, making it possible to realize a quantum $\mathcal{APT}$-symmetry without Langevin noises [36–38]. In this Letter, we construct a quantum $\mathcal{APT}$-symmetry in a two-mode bosonic system, where the dynamical Hamiltonian matrix is non-Hermitian and preserves the $\mathcal{APT}$-symmetry, while the second-quantized Hamiltonian is Hermitian. In this sense, we name it a pseudo-$\mathcal{APT}$ symmetry. Our main results are:

i) The quantum pseudo-$\mathcal{APT}$-symmetry builds on coupling Bose creation operator of one field with the annihilation operator of the other field, yielding the Hermiticity of the second-quantized Hamiltonian that does not involve Langevin noises. The spontaneous $\mathcal{APT}$ symmetry breaking across the EP for the dynamical Hamiltonian matrix yields a transition from purely imaginary ($\mathcal{APT}$-symmetric) to purely real ($\mathcal{APT}$-broken) eigenvalues, which is opposite to typical real to imaginary transition for the $\mathcal{PT}$-symmetry.

ii) Across the EP, the pseudo-$\mathcal{APT}$ symmetry and quantized Hamiltonian yield a transition between different types of quantum squeezing dynamics. Specifically, the two-mode squeezing factor oscillates periodically with time in the pseudo-$\mathcal{APT}$-broken region, increases linearly at EP, and grows exponentially in the pseudo-$\mathcal{APT}$-symmetric region. Optical field squeezed states have been widely studied because of their fundamental interest (e.g., the implementation of EPR paradox) as well as broad applications in quantum information processing (e.g., continuous-variable quantum teleportation) and quantum metrology (e.g., gravitational wave detection) [39, 40]. Here the connection between pseudo-$\mathcal{APT}$-symmetry transition and different quantum squeezing dynamics is established.

iii) The dramatic changes of quantum squeezing factors and dynamics close to the EP make them ultrasensitive to some parameters, thus can be utilized to achieve ultra-precision quantum sensing. In contrast to quantum sensing based on large squeezing factor [41, 42], here we focus on the $\mathcal{APT}$-broken region with weak squeezing that is usually undesirable in previous experi-

ments. We show that simple measurement schemes can reach the sensitivity close to the quantum Cramér-Rao bound given by the quantum Fisher information [41, 42], which exhibits divergent feature as the EP is approached. The squeezing factor is 1 at the working points, therefore the ultra-precision sensitivity originates from the pseudo-$\mathcal{APT}$ symmetry rather than squeezing or entanglement.

iv) We propose that the connection between the quantum pseudo-$\mathcal{APT}$ symmetry and the transition of squeezing dynamics as well as the ultra-precision quantum sensors can be realized experimentally in spontaneous wave mixing nonlinear optics and ultracold atomic Bose-Einstein condensates (BECs). In the BEC case, we establish the connection between the pseudo-$\mathcal{APT}$ transition and the well-known transition to dynamical instability [43].

Pseudo-$\mathcal{APT}$-symmetry and quantum squeezing.— Consider a two-mode bosonic model described by the second-quantized Hermitian Hamiltonian

$$\mathcal{H} = \delta\left(\hat{a}_1^\dagger\hat{a}_1 + \hat{a}_2^\dagger\hat{a}_2\right) + i\kappa\left(\hat{a}_1^\dagger\hat{a}_2^\dagger - \hat{a}_1\hat{a}_2\right), \qquad (1)$$

where $\hat{a}_j$ and $\hat{a}_j^\dagger$ are the bosonic annihilation and creation operators, and the detuning δ and coupling coefficient κ are both real numbers. From Heisenberg equation, we obtain the dynamical equation (we set $\hbar = 1$) [44]

$$i\partial_t\left(\hat{a}_1,\ \hat{a}_2^\dagger\right)^T = H_{APT}\left(\hat{a}_1,\ \hat{a}_2^\dagger\right)^T, \qquad (2)$$

with the non-Hermitian dynamical Hamiltonian matrix

$$H_{APT} = \delta\sigma_z + i\kappa\sigma_x = \begin{pmatrix} \delta & i\kappa \\ i\kappa & -\delta \end{pmatrix}. \qquad (3)$$

H_{APT} satisfies $\{H_{APT}, \mathcal{PT}\} = 0$, with the parity operator $\mathcal{P} = \sigma_x$ and the time-reversal complex conjugate operator $\mathcal{T}$. In the pseudo-$\mathcal{APT}$-symmetric region (*i.e.*, the eigenstates of H_{APT} are $\mathcal{PT}$-symmetric) $|\delta| < |\kappa|$, H_{APT} has two imaginary eigenvalues $\lambda_\pm = \pm i\lambda_0$ with $\lambda_0 = \sqrt{|\kappa^2 - \delta^2|}$ [44]. While in the pseudo-$\mathcal{APT}$-broken region $|\delta| > |\kappa|$, H_{APT} has two real eigenvalues $\lambda_\pm = \pm\lambda_0$. The spontaneous symmetry breaking occurs at the EP $|\kappa| = |\delta|$, where $\lambda_0 = 0$. In the classical limit, the field operators $\hat{a}_1$ and $\hat{a}_2^\dagger$ are replaced by complex numbers, and the model reduces to the non-Hermitian system with $\mathcal{APT}$ symmetry [36, 37]. In the quantum realm, we name it as pseudo-$\mathcal{APT}$ symmetry in the sense that H_{APT} is non-Hermitian while $\mathcal{H}$ is Hermitian.

The field operators at time t can be obtained from the dynamical equation (2) as [44]

$$\hat{a}_j(t) = A\hat{a}_j(0) + B\hat{a}_{\bar{j}}^\dagger(0), \qquad (4)$$

where $\bar{j}$ represents the different mode number from j. In the pseudo-$\mathcal{APT}$-broken (symmetric) region, we have $A = \cos(\lambda_0 t) - i\frac{\delta}{\lambda_0}\sin(\lambda_0 t)$ ($A = \cosh(\lambda_0 t) - i\frac{\delta}{\lambda_0}\sinh(\lambda_0 t)$) and $B = \frac{\kappa}{\lambda_0}\sin(\lambda_0 t)$ ($B = \frac{\kappa}{\lambda_0}\sinh(\lambda_0 t)$). $|A|^2 - |B|^2 = 1$ in both regions and the bosonic commutation relations $[\hat{a}_j(t), \hat{a}_{j'}^\dagger(t)] = [\hat{a}_j(0), \hat{a}_{j'}^\dagger(0)] = \delta_{jj'}$ are preserved without Langevin noises [44].

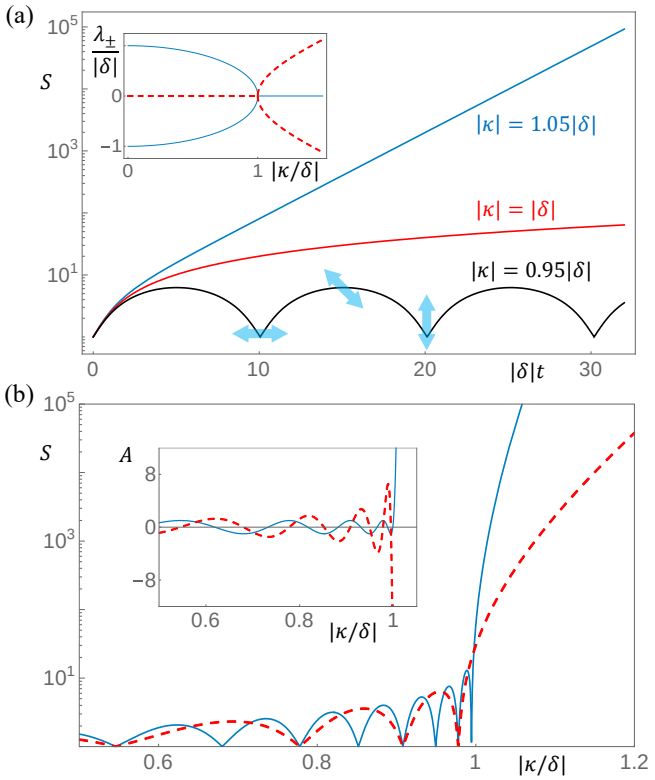

FIG. 1. Pseudo-$\mathcal{APT}$ symmetry induced quantum squeezing dynamics. (a) The squeezing factor versus evolution time for different κ. $|\kappa/\delta| = 0.95, 1$ and 1.05 correspond to pseudo-$\mathcal{APT}$ broken, EP and pseudo-$\mathcal{APT}$ symmetric regions, respectively. Blue arrows indicate the two-mode squeezing directions for $\kappa, \delta > 0$. The inset shows the eigenvalues of H_{APT}. Solid (dashed) lines are the real (imaginary) parts. (b) Squeezing factor versus κ for different evolution time. Solid (dashed) line corresponds to $|\delta|t = 30$ ($|\delta|t = 15$). Inset shows A versus $|\kappa/\delta|$ with $|\delta|t = 30$. Solid (dashed) line is the real (imaginary) part. $B = -\kappa\mathrm{Im}[A]/\delta$.

The two-mode quantum squeezed states are generated from the terms $\hat{a}_1^\dagger\hat{a}_2^\dagger - \hat{a}_1\hat{a}_2$ in $\mathcal{H}$ and can be characterized by the quadrature operators $\hat{X}_j(\varphi, t) = [e^{-i\varphi}\hat{a}_j(t) + h.c.]/2$ of the two modes, which satisfy $\hat{X}_1(\varphi_+, t) \pm \hat{X}_2(\varphi_+, t) = S^{\pm 1}[\hat{X}_1(\varphi_-, 0) \pm \hat{X}_2(\varphi_-, 0)]$. Here $A = A_0 e^{i\varphi_A}$ and $B = B_0 e^{i\varphi_B}$ with the positive amplitudes $A_0^2 - B_0^2 = 1$, $S = A_0 + B_0 \geq 1$ is the two-mode squeezing factor, $\varphi_+ = (\varphi_B + \varphi_A)/2$ is the squeezing angle. The angle $\varphi_- = (\varphi_B - \varphi_A)/2$ is not important because the initial state is usually unentangled and isotropic (e.g. the vacuum or coherent state).

Fig. 1 shows the transition between different types of quantum squeezing behaviors with the pseudo-$\mathcal{APT}$ symmetry starting from an initial vacuum or coherent

state. In the pseudo-$\mathcal{APT}$-symmetric region ($|\kappa/\delta| > 1$), one of the eigenmodes disappears after a long time evolution due to purely imaginary $\lambda_\pm$, therefore $A_0 \simeq B_0 \simeq \frac{\kappa}{2\lambda_0} e^{\lambda_0 t}$ at the long time and $S \simeq \frac{\kappa}{\lambda_0} e^{\lambda_0 t}$ grows exponentially. The squeezing angle ϕ_+ quickly changes from $\frac{1}{2}\mathrm{Arg}[\kappa]$ to its saturated value $\frac{1}{2}\mathrm{Arg}[\kappa\lambda_0 - i\kappa\delta]$. In the pseudo-$\mathcal{APT}$-broken region, S shows oscillating behavior with a period $T = \pi/\lambda_0$, going back to 1 (non-squeezing) at $t = nT$ and reaching the maximum $S_{\max} = \sqrt{(|\delta| + |\kappa|)/(|\delta| - |\kappa|)}$ at $t = (n + 1/2)T$ (n is an integer). In each period starting from $S = 1$, φ_+ changes from $\frac{1}{2}\mathrm{Arg}[\kappa]$ to $\frac{1}{2}\mathrm{Arg}[-i\kappa\delta]$ as S increases to the maximum, and then to $\frac{1}{2}\mathrm{Arg}[-\kappa]$ as S decreases to 1, as schematically illustrated in Fig. 1a. At the EP, two eigenmodes coalesce to a single mode. We have $A = 1 - i\delta t$, $B = \kappa t$ [44], and $S = \sqrt{1 + \delta^2 t^2} + |\kappa| t$ increases linearly at long time $|\delta| t \gg 1$. φ_+ changes monotonically from $\frac{1}{2}\mathrm{Arg}[\kappa]$ to $\frac{1}{2}\mathrm{Arg}[-i\kappa\delta]$. The results at the EP are consistent with the $|\kappa| \to |\delta|$ limit from both sides.

Since the squeezing behaviors change dramatically across the EP, the dynamical quantum state at a given time should also be sensitive to the system parameters δ, κ around the EP. In Fig. 1b, we plot S as a function of $|\kappa/\delta|$ at different times. We see S oscillates with increasing amplitude and frequency as $|\kappa|$ is approaching the EP. Near the EP, the squeezing factor (thereby the quantum state) exhibits a sharp change around $S = 1$ (*i.e.*, for κ satisfying $\lambda_0 t = n\pi$), where the system returns to its initial non-squeezing quantum state. The coefficients A and B show similar oscillation behaviors as S (the inset of Fig. 1b). Such critical behavior around the EP can be utilized to implement ultra-precision quantum sensing.

Quantum sensing.—Precision measurements are long pursued due to their vital importance in physics and many other sciences. Quantum sensing, such as large squeezing factor state, quantum entanglement [41, 42], and phase-transition criticality based sensors [54–59], utilize unique quantum phenomena for ultra-precision measurements. Recent studies showed that the EPs of the $\mathcal{PT}$-symmetry can enhance the optical sensing in the classical region [60]. Here we explore ultra-precision quantum sensing enabled by the quantum pseudo-$\mathcal{APT}$-symmetry without Langevin noises.

We focus on the pseudo-$\mathcal{APT}$-broken region $|\kappa| < |\delta|$ (see [44] for discussions on the region $|\kappa| > |\delta|$), which is dynamical stable without the exponential growth of excitations. We propose a simple scheme to measure A and B directly, which are sensitive to the system parameters κ, δ and thus can be used to sense κ and δ. The sensing precision is at the same order as quantum Cramér-Rao bound set by the quantum Fisher information of the quantum state, which shows divergent feature close to the EP.

We consider a coherent initial state $|\psi_0\rangle = |\alpha_1, \alpha_2\rangle$ of two bosonic modes for the quantum sensor. After an evolution time t, we perform the quadrature measurement $\hat{X}_j(0,t)$ of the final states using standard homodyne detection [61], which give the mean value and variance

$$\langle \hat{X}_j(0,t)\rangle_{\psi_0} = \mathrm{Re}[A\alpha_j + B\alpha_{\bar{j}}^*] \tag{5}$$

$$[\Delta \hat{X}_j(0,t)]^2 = \frac{1}{4}(A_0^2 + B_0^2), \tag{6}$$

with $\bar{j} \neq j$. Therefore we can determine A and B from the measurement results for the estimation of κ or δ. Without loss of generality, we choose $\kappa\delta > 0$ and set $\alpha_2 = -i\alpha_1 \equiv \alpha$ (different choices of parameters α_i give similar results, which do not affect the sensing precision). In Fig. 2a, we plot the observable $\langle \hat{X}_1(0,t)\rangle_{\psi_0} = \alpha \sin(\lambda_0 t)\frac{\kappa+\delta}{\lambda_0}$ as a function of κ with fixed δ and t, which possesses strong and fast oscillation close to the EP. Such oscillation becomes more pronounced as the evolution time increases.

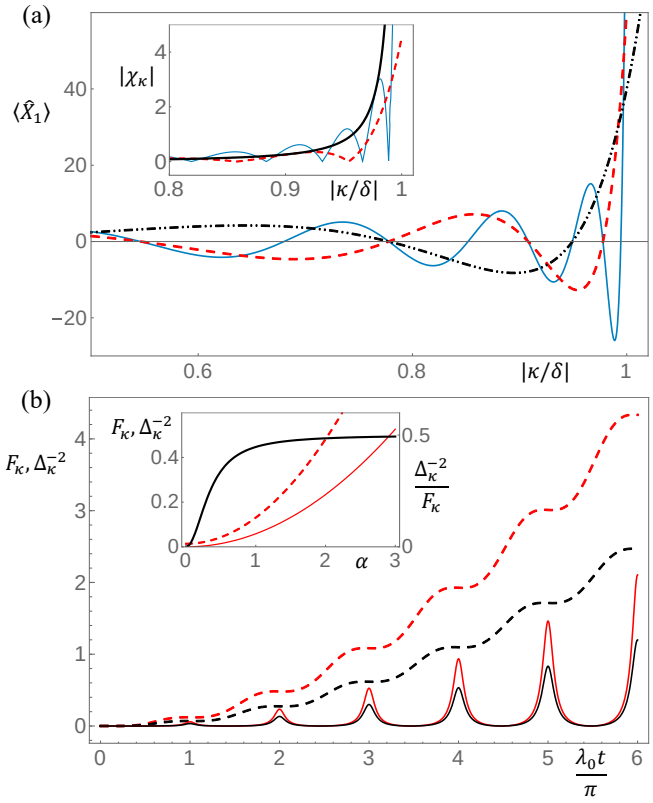

FIG. 2. Quantum sensing based on pseudo-$\mathcal{APT}$ symmetry. (a) The quadrature $\langle \hat{X}_1 \rangle$ versus κ at different evolution time, with $\alpha = 2 \cdot \mathrm{sign}(\delta)$. $|\delta| t = 10, 15$ and 30 are shown by the dash-dotted, dashed and solid lines, respectively. Inset shows the corresponding susceptibility $|\chi_\kappa|$ (in unit of 10^3), with bold solid line showing the results with κ-dependent time satisfying $\lambda_0 t = 2\pi$. The working points are located near $\langle \hat{X}_1 \rangle = 0$ (i.e., the maxima of χ_κ). (b) The inverse variance Δ_κ^{-2} (solid lines) of the observable and the quantum Fisher information F_κ (dashed lines) as functions of evolution times (in unit of 10^7) with $\alpha = 2$. Red and black lines are for $\kappa/\delta = 0.95$ and 0.94, respectively. Local maxima of Δ_κ^{-2} give the work points $\lambda_0 t = n\pi$. Inset shows the results as functions of α for $\lambda_0 t = 2\pi$ and $\kappa/\delta = 0.95$, with bold black line corresponding to $\Delta_\kappa^{-2}/F_\kappa$.

The measurement of the change of $\langle \hat{X}_j(0,t)\rangle_{\psi_0}$ with κ gives the susceptibility $\chi_\kappa(t) \equiv \partial_\kappa \langle \hat{X}_1(0,t)\rangle_{\psi_0}$ which exhibits divergent feature close to the EP $\kappa \to \delta$ (*i.e.*, $\lambda_0 \to 0$). Similar results apply to the susceptibility with δ. In Fig. 2a, we plot χ_κ for a fixed evolution time as well as the sensor working point $t = nT$. The later one possesses a divergent scaling $\chi_\kappa(nT) = -\alpha \frac{\kappa(\kappa+\delta)n\pi}{\lambda_0^3} \sim \lambda_0^{-3}$. Longer evolution time is required for smaller λ_0 to observe such divergence. Note that the eigenvalues of H_{APT} have a square-root splitting with divergent sensitivity $\partial_\kappa \lambda_0 = -\frac{\kappa}{\lambda_0}$ close to the EP. In addition, the eigenmodes are not orthogonal and coalesce at the EP, which are responsible for the factor λ_0^{-1} in the final Bosonic field $\hat{a}_j(t)$. Together they give the divergent scaling $\chi_\kappa(t) \sim \lambda_0^{-3}$ for an evolution time $t \sim \lambda_0{}^{-1}$.

The precision of the parameter estimation of κ is given by the variance $\Delta_\kappa^2 = [\Delta \hat{X}_1]^2/\chi_\kappa^2$, and the performance of the sensing scheme can be evaluated by comparing the inverse variance Δ_κ^{-2} with the quantum Fisher information F_κ, whose inverse gives the ultimate precision for quantum sensing, *i.e.*, reaching quantum Cramér-Rao bound $\Delta_\kappa^{-2} \leq F_\kappa$ (optimal measurement is usually required). For the coherent initial state $|\psi_0\rangle$,

$$F_\kappa(t) = 4A_0^4 |\partial_\kappa \frac{B}{A^*}|^2 + 4(A_0^2 + B_0^2) \sum_j |\partial_\kappa \langle \hat{a}_j(t)\rangle_{\psi_0}|^2 \\ -16\Re[A^* B^* \partial_\kappa \langle \hat{a}_1(t)\rangle_{\psi_0} \partial_\kappa \langle \hat{a}_2(t)\rangle_{\psi_0}] \tag{7}$$

after the evolution time t [44]. In Fig. 2b, we compare Δ_κ^{-2} with F_κ at different evolution times. We see that Δ_κ^{-2} has some narrow peaks when κ satisfies $t = nT$ (*i.e.*, the variance Δ_κ reaches the minimum) for fixed δ and $|\kappa| \lesssim |\delta|$, while $F_\kappa(t)$ smoothly increases with κ and takes larger values for all κ near the EP. At working points $t = nT$, $F_\kappa(nT) = \left[8 + \frac{4\kappa^2}{\alpha^2(\kappa+\delta)^2}\right] \chi_\kappa^2 \sim \lambda_0^{-6}$, while $\Delta_\kappa^{-2}(nT) = 4\chi_\kappa^2 \simeq 0.5 F_\kappa$ for coherent amplitudes α that are not too weak (e.g., $\alpha \sim 2$), as shown in Fig. 2b. During the evolution, the number of bosonic excitations $N \sim \lambda_0^{-2}$, therefore $\Delta_\kappa^{-2} \sim N^2 t^2$, which is at the same order as the Heisenberg limit.

Notice that at the working points $t = nT$, the squeezing factor $S = 1$, therefore the ultra-precision sensitivity originates from the pseudo-$\mathcal{APT}$ symmetry breaking, making our scheme distinct from traditional quantum sensors based on large squeezing factors.

Experimental realization.—The quantum pseudo-$\mathcal{APT}$ symmetry physics can be realized in quantum optics systems or atomic BECs. In the quantum optics implementation, we can utilize nonlinear wave mixing such as spontaneous parametric down conversion (SPDC) [62, 63] and spontaneous four-wave mixing (SFWM) [64, 65] with carefully designed parameters. A schematic illustration of the optical setup is shown in Fig. 3a and more detailed studies are provided in [44]. In SFWM, two quantum modes ($\hat{a}_{1,2}$) copropagate along the z direction in the nonlinear optical medium and are coupled through a nonlinear coupling coefficient κ which can be tuned by changing two additional pump lasers' intensity and frequency, as well as the material properties. The parameter δ is associated with the phase mismatching $\delta = -\Delta k/2$ depending on laser frequency and propagation direction, where $\Delta k = (\mathbf{k}_1 + \mathbf{k}_2 - \sum \mathbf{k}_{\text{pump}}) \cdot \hat{\mathbf{z}}$ with $\mathbf{k}_j$ being the wave vectors and $\hat{\mathbf{z}}$ the unit vector. In this system, the propagation along the z direction simulates the time evolution in our theoretical model (*i.e.*, $t = z$). In the quantum sensing, the final output quantum fields of two modes from the nonlinear medium will be measured using standard homodyne detection, yielding the mean value and variance of quadratures of two modes.

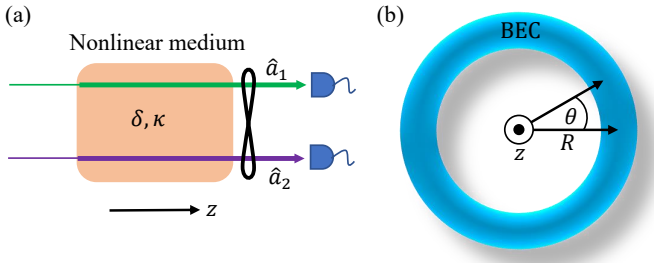

FIG. 3. Experimental implementations. (a) Schematic optical setup for realizing pseudo-$\mathcal{APT}$ symmetry physics through nonlinear spontaneous four-wave mixing. (b) Experimental realization based on a cold atomic BEC in a ring trap.

In the atomic implementation, we consider a BEC in a ring dipole trap (as shown in Fig. 3b) with a strong confinement along z and radial directions, which can be realized by Laguerre-Gaussian lasers as demonstrated in recent experiments [66, 67]. The dynamics are reduced to one dimension (*i.e.*, the azimuthal angle θ). We can expand the BEC field operator in the angular momentum space as [68, 69]

$$\hat{\Psi}(\theta, t) = e^{-i\mu t - i\pi/4} \Phi(t) + e^{-i\mu t} \sum_{n \neq 0} \hat{\psi}_n(t) \frac{e^{in\theta}}{\sqrt{2\pi}}, \tag{8}$$

where Φ is the condensate wave function (Φ is real initially and $\pi/4$ is a gauge choice), $\mu = -g|\Phi|^2 - g\sum_n \langle \psi_n^\dagger \psi_n \rangle / 2\pi$ is the chemical potential, and g is the interaction strength ($g > 0$ corresponds to attractive interaction). The quantum excitation operators $\hat{\psi}_n(t)$ satisfy the Bogoliubov equation [44]

$$i\partial_t \begin{pmatrix} \hat{\psi}_n \\ \hat{\psi}_{-n}^\dagger \end{pmatrix} = \begin{pmatrix} \delta_n & i\kappa \\ i\kappa^* & -\delta_n \end{pmatrix} \begin{pmatrix} \hat{\psi}_n \\ \hat{\psi}_{-n}^\dagger \end{pmatrix}, \tag{9}$$

which shares the same form as Eq. 2. Here $\delta_n = n^2 E_1 - g|\Phi|^2$, $\kappa = g\Phi^2$, and $E_1 = \frac{1}{2mR^2}$ is the kinetic energy of the first excited state along the ring with radius R. At $g = 0$, the quantum pseudo-$\mathcal{APT}$ symmetry is broken for all n. As g increases, the BEC becomes dynamical unstable when $2g|\Phi|^2 > E_1$ (i.e., $|\kappa| > |\delta_1|$),

where the pseudo-$\mathcal{APT}$ symmetry is restored for $n = 1$, and the excitation number and squeezing factor grow exponentially [70, 71]. For the quantum sensing, we can first prepare the BEC to its ground state with $g \simeq 0$. The initial coherent state for $n = \pm 1$ can be generated by Raman process with Laguerre-Gaussian beams carrying ± 1 orbital angular momentum. Then we increase g to the working point near the EP (*i.e.*, $2g|\Phi|^2 = E_1$). The quadratures $\hat{X}_n$, which is proportional to the visibility of the density modulation along θ, can be measured by density imaging. The performance of the sensor is very similar as that shown in Fig. 2 [44]. We want to point out that the Kerr interaction of photons as well as the interaction between excitations of the BEC are extremely weak, which can hardly affect the finite duration dynamics of interest [44].

Conclusion.—In summary, we construct a quantum pseudo-$\mathcal{APT}$ symmetry without Langevin noises and show that its transition across EP yields a dramatic change of quantum squeezed dynamics. The divergent sensitivity of squeezed states close to the EP can be utilized for ultra-precision sensing approaching the quantum limit. The experimental realization of such quantum pseudo-$\mathcal{APT}$ symmetry in nonlinear quantum optical wave mixing and ultracold atomic BECs will provide realistic platforms for studying quantum non-Hermitian physics and its quantum sensing applications. The two-mode quantum pseudo-$\mathcal{APT}$ symmetry can also be generalized to a multi-mode system supporting higher-order EPs [72, 73], which may lead to novel symmetry breaking physics and even higher sensing precision.

Acknowledgments.—X.W.L. and C.Z. acknowledge support from NSF (PHY-2110212), ARO (W911NF17-1-0128), and AFOSR (FA9550-20-1-0220,FA9550-22-1-0043). S.D. acknowledges support from DOE (DE-SC0022069).

* Chuanwei.Zhang@utdallas.edu
† dusw@utdallas.edu

[1] C. M. Bender and S. Boettcher, Real Spectra in Non-Hermitian Hamiltonians Having $\mathcal{PT}$ Symmetry, Phys. Rev. Lett. **80**, 5243 (1998).
[2] C. M. Bender, Making sense of non-Hermitian Hamiltonians, Rep. Prog. Phys. **70**, 947 (2007).
[3] R. El-Ganainy, K. G. Makris, M. Khajavikhan, Z. H. Musslimani, S. Rotter, and D. N. Christodoulides, Non-Hermitian physics and PT symmetry, Nat. Phys. **14**, 11 (2018).
[4] Ş. K. Özdemir, S. Rotter, F. Nori, and L. Yang, Parity-time symmetry and exceptional points in photonics, Nat. Mater. **18**, 783 (2019).
[5] M.-A. Miri and A. Alù, Exceptional points in optics and photonics, Science **363**, 1457 (2019).
[6] V. V. Konotop, J. Yang, and D. A. Zezyulin, Nonlinear waves in $\mathcal{PT}$-symmetric systems, Rev. Mod. Phys. **88**, 035002 (2016).
[7] L. Feng, R. El-Ganainy and L. Ge, Non-Hermitian photonics based on parity–time symmetry, Nat. Photonics **11**, 752 (2017).
[8] R. El-Ganainy, K. G. Makris, D. N. Christodoulides, and Z. H. Musslimani, Theory of coupled optical PT-symmetric structures, Opt. Lett. **32**, 2632 (2007).
[9] A. Guo, G. J. Salamo, D. Duchesne, R. Morandotti, M. Volatier-Ravat, V. Aimez, G. A. Siviloglou, and D. N. Christodoulides, Observation of $\mathcal{PT}$-Symmetry Breaking in Complex Optical Potentials, Phys. Rev. Lett. **103**, 093902 (2009).
[10] C. E. Rüter, K. G. Makris, R. El-Ganainy, D. N. Christodoulides, M. Segev, and D. Kip, Observation of parity-time symmetry in optics, Nat. Phys. **6**, 192 (2010).
[11] B. Peng, Ş. K. Özdemir, F. Lei, F. Monifi, M. Gianfreda, G. L. Long, S. Fan, F. Nori, C. M. Bender, and L. Yang, Parity–time-symmetric whispering-gallery microcavities, Nat. Phys. **10**, 394 (2014).
[12] C. Hang, G. Huang, and V. V. Konotop, $\mathcal{PT}$ Symmetry with a System of Three-Level Atoms, Phys. Rev. Lett. **110**, 083604 (2013).
[13] Z. Zhang, Y. Zhang, J. Sheng, L. Yang, M.-A. Miri, D. N. Christodoulides, B. He, Y. Zhang, and M. Xiao, Observation of Parity-Time Symmetry in Optically Induced Atomic Lattices, Phys. Rev. Lett. **117**, 123601 (2016).
[14] J. Schindler, A. Li, M. C. Zheng, F. M. Ellis, and T. Kottos, Experimental study of active LRC circuits with $\mathcal{PT}$ symmetries, Phys. Rev. A **84**, 040101 (2011).
[15] R. Fleury, D. Sounas, and A. Alù, An invisible acoustic sensor based on parity-time symmetry, Nat. Commun. **6**, 5905 (2015).
[16] X. Zhu, H. Ramezani, C. Shi, J. Zhu, and X. Zhang, $\mathcal{PT}$-Symmetric Acoustics, Phys. Rev. X **4**, 031042 (2014).
[17] L. Feng, Z. J. Wong, R.-M. Ma, Y. Wang, and X. Zhang, Single-mode laser by parity-time symmetry breaking, Science **346**, 972 (2014).
[18] H. Hodaei, M.-A. Miri, M. Heinrich, D. N. Christodoulides, and M. Khajavikhan, Parity-time–symmetric microring lasers, Science **346**, 975 (2014).
[19] J. Wiersig, Enhancing the Sensitivity of Frequency and Energy Splitting Detection by Using Exceptional Points: Application to Microcavity Sensors for Single-Particle Detection, Phys. Rev. Lett. **112**, 203901 (2014).
[20] Z.-P. Liu, J. Zhang, Ş. K. Özdemir, , B. Peng, H. Jing, X.-Y. Lü, C.-W. Li, L. Yang, F. Nori, and Y.-X. Liu, Metrology with $\mathcal{PT}$-Symmetric Cavities: Enhanced Sensitivity near the $\mathcal{PT}$-Phase Transition, Phys. Rev. Lett. **117**, 110802 (2016).
[21] Y. Choi, C. Hahn, J. W. Yoon, S. H. Song, and P. Berini, Extremely broadband, on-chip optical nonreciprocity enabled by mimicking nonlinear anti-adiabatic quantum jumps near exceptional points, Nat. Commun. **8**, 14154 (2017).
[22] H.-K. Lau and A. A. Clerk, Fundamental limits and non-reciprocal approaches in non-Hermitian quantum sensing, Nat. Commun. **9**, 4320 (2018).
[23] M. Zhang, W. Sweeney, C. W. Hsu, L. Yang, A. D. Stone, and L. Jiang, Quantum Noise Theory of Exceptional Point Amplifying Sensors, Phys. Rev. Lett. **123**, 180501 (2019).
[24] Y. Chu, Y. Liu, H. Liu, and J. Cai, Quantum Sens-

ing with a Single-Qubit Pseudo-Hermitian System, Phys. Rev. Lett. **124**, 020501 (2020).
[25] M. Naghiloo, M. Abbasi, Y. N. Joglekar, and K. W. Murch, Quantum state tomography across the exceptional point in a single dissipative qubit, Nat. Phys. **15**, 1232 (2019).
[26] Y. Wu, et al. Observation of parity-time symmetry breaking in a single-spin system, Science **364**, 878 (2019).
[27] Yu, S. et al. Experimental Investigation of Quantum PT -Enhanced Sensor. Phys. Rev. Lett. **125**, 240506 (2020).
[28] S. Scheel and A. Szameit, PT-symmetric photonic quantum systems with gain and loss do not exist, Europhysics Lett. **122**, 34001 (2018).
[29] L. Ge and H. E. Türeci, Antisymmetric $\mathcal{PT}$-photonic structures with balanced positive- and negative-index materials, Phys. Rev. A **88**, 053810 (2013).
[30] P. Peng, W. Cao, C. Shen, W. Qu, J. Wen, L. Jiang, and Y. Xiao, Anti-parity-time symmetry with flying atoms, Nat. Phys. **12**, 1139 (2016).
[31] J.-H. Wu, M. Artoni, and G. C. La Rocca, Non-Hermitian Degeneracies and Unidirectional Reflectionless Atomic Lattices, Phys. Rev. Lett. **113**, 123004 (2014).
[32] F. Yang, Y.-C. Liu, and L. You, Anti-$\mathcal{PT}$ symmetry in dissipatively coupled optical systems, Phys. Rev. A **96**, 053845 (2017).
[33] V. V. Konotop and D. A. Zezyulin, Odd-Time Reversal $\mathcal{PT}$ Symmetry Induced by an Anti-$\mathcal{PT}$-Symmetric Medium, Phys. Rev. Lett. **120**, 123902 (2018).
[34] X.-L. Zhang, S. Wang, B. Hou, and C. T. Chan, Dynamically Encircling Exceptional Points: In situ Control of Encircling Loops and the Role of the Starting Point, Phys. Rev. X **8**, 021066 (2018).
[35] Y. Li, Y.-G. Peng, L. Han, M.-A. Miri, W. Li, M. Xiao, X.-F. Zhu, J. Zhao, A. Alù, S. Fan, and C.-W. Qiu, Anti-parity-time symmetry in diffusive systems, Science **364**, 170 (2018).
[36] Y. Jiang, Y. Mei, Y. Zuo, Y. Zhai, Jensen Li, J. Wen, and S. Du, Anti-Parity-Time Symmetric Optical Four-Wave Mixing in Cold Atoms, Phys. Rev. Lett. **123**, 193604 (2019).
[37] M.-A. Miri and A. Alù, Nonlinearity-induced PT-symmetry without material gain, New J. Phys. **18**, 065001 (2016).
[38] Y.-X. Wang and A. A. Clerk, Non-Hermitian dynamics without dissipation in quantum systems, Phys. Rev. A **99**, 063834 (2019).
[39] S. L. Braunstein and P. van Loock, Quantum information with continuous variables, Rev. Mod. Phys. **77**, 513 (2005).
[40] A. I. Lvovsky, Squeezed light, Photon. Sci. Found., Technol. Appl. **1**, 121 (2015).
[41] V. Giovannetti, S. Lloyd, and L. Maccone, Advances in quantum metrology, Nat. Photon. **5**, 222 (2011).
[42] L. Pezzè, A. Smerzi, M. K. Oberthaler, R. Schmied, and P. Treutlein, Quantum metrology with nonclassical states of atomic ensembles, Rev. Mod. Phys. **90**, 035005 (2018).
[43] H. Smith and C. J. Pethick, BoseEinstein Condensation in Dilute Gases, Cambridge University Press, (2001).
[44] See Supplementary Materials for more information about the squeezing properties, quantum Fisher information, implementation with quantum optics and BEC, and Kerr nonlinearity with Refs. [45–53].
[45] N. Bartolo, F. Minganti, W. Casteels, and C. Ciuti, Exact steady state of a Kerr resonator with one- and two-photon driving and dissipation: Controllable Wigner-function multimodality and dissipative phase transitions, Phys. Rev. A **94**, 033841 (2016).
[46] P. Krantz, A. Bengtsson, M. Simoen, S. Gustavsson, V. Shumeiko, W. D. Oliver, C. M. Wilson, P. Delsing, and J. Bylander, Single-shot read-out of a superconducting qubit using a Josephson parametric oscillator, Nat. Commun. **7**, 11417 (2016).
[47] F. Minganti, A. Biella, N. Bartolo, and C. Ciuti, Spectral theory of Liouvillians for dissipative phase transitions, Phys. Rev. A **98**, 042118 (2018).
[48] T. L. Heugel, M. Biondi, O. Zilberberg, and R. Chitra, Quantum Transducer Using a Parametric Driven-Dissipative Phase Transition, Phys. Rev. Lett. **123**, 173601 (2019).
[49] S. Lieu, R. Belyansky, J. T. Young, R. Lundgren, V. V. Albert, and A. V. Gorshkov, Symmetry Breaking and Error Correction in Open Quantum Systems, Phys. Rev. Lett. **125**, 240405 (2020).
[50] Xin H. H. Zhang and Harold U. Baranger, Driven-dissipative phase transition in a Kerr oscillator: From semiclassical $\mathcal{PT}$ symmetry to quantum fluctuations, Phys. Rev. A **103**, 033711 (2021).
[51] R. Di Candia, F. Minganti, K. V. Petrovnin, G. S. Paraoanu, and S. Felicetti, Critical parametric quantum sensing, arXiv:2107.04503.
[52] D. G. Fried, T. C. Killian, L. Willmann, D. Landhuis, S. C. Moss, D. Kleppner, and T. J. Greytak, Bose-Einstein Condensation of Atomic Hydrogen, Phys. Rev. Lett. **81**, 3811 (1998).
[53] N. P. Robins, P. A. Altin, J. E. Debs, and J. D. Close, Atom lasers: Production, properties and prospects for precision inertial measurement, Phys. Rep. **529**, 265 (2013).
[54] M. Tsang, Quantum transition-edge detectors, Phys. Rev. A **88**, 021801 (2013).
[55] M. Skotiniotis, P. Sekatski, and W. Dür, Quantum metrology for the Ising Hamiltonian with transverse magnetic field, New J. Phys. **17**, 073032 (2015).
[56] K. Macieszczak, M. Guţă, I. Lesanovsky, and J. P. Garrahan, Dynamical phase transitions as a resource for quantum enhanced metrology, Phys. Rev. A **93**, 022103 (2016).
[57] Y. Chu, S. Zhang, B. Yu, and J. Cai, Dynamic Framework for Criticality-Enhanced Quantum Sensing, Phys. Rev. Lett. **126**, 010502 (2021).
[58] L. Garbe, M. Bina, A. Keller, M. G. A. Paris, and S. Felicetti, Critical Quantum Metrology with a Finite-Component Quantum Phase Transition, Phys. Rev. Lett. **124**, 120504 (2020).
[59] M. M. Rams, P. Sierant, O. Dutta, P. Horodecki, and J. Zakrzewski, At the Limits of Criticality-Based Quantum Metrology: Apparent Super-Heisenberg Scaling Revisited, Phys. Rev. X **8**, 021022 (2018).
[60] J. Wiersig, Review of exceptional point-based sensors, Photon. Res. **8**, 1457 (2020).
[61] H. M. Wiseman and G. J. Milburn, Quantum Measurement and Control (Cambridge University Press, Cambridge, 2010).
[62] S. E. Harris, M. K. Oshman, and R. L. Byer, Observation of Tunable Optical Parametric Fluorescence, Phys. Rev. Lett. **18**, 732 (1967).
[63] D. N. Klyshko, A. N. Penin, and B. F. Polkovnikov, Parametric Luminescence and Light Scattering by Polaritons,

JETP Lett. **11**, 05 (1970).
[64] S. Du, J. Wen, and M. H. Rubin, Narrowband biphoton generation near atomic resonance, J. Opt. Soc. Am. B **25**, C98 (2008).
[65] L. Zhao, Y. Su, and S. Du, Narrowband biphoton generation in the group delay regime, Phys. Rev. A **93**, 033815 (2016).
[66] O. Morizot, Y. Colombe, V. Lorent, H. Perrin, and B. M. Garraway, Ring trap for ultracold atoms, Phys. Rev. A **74**, 023617 (2006).
[67] S. Eckel, J. G. Lee, F. Jendrzejewski, N. Murray, C. W. Clark, C. J. Lobb, W. D. Phillips, M. Edwards, and G. K. Campbell, Hysteresis in a quantized superfluid atomtronic circuit, Nature **506**, 200 (2014).
[68] A. Griffin, Conserving and gapless approximations for an inhomogeneous Bose gas at finite temperatures, Phys. Rev. B **53**, 9341 (1996).
[69] R. Ozeri, N. Katz, J. Steinhauer, and N. Davidson, Colloquium: Bulk Bogoliubov excitations in a Bose-Einstein condensate, Rev. Mod. Phys. **77**, 187 (2005).
[70] V. A. Yurovsky, Quantum effects on dynamics of instabilities in Bose-Einstein condensates, Phys. Rev. A **65**, 033605 (2002).
[71] E. A. Calzetta and B. L. Hu, Bose-Einstein condensate collapse and dynamical squeezing of vacuum fluctuations, Phys. Rev. A **68**, 043625 (2003).
[72] H. Hodaei, A. U. Hassan, S. Wittek, H. Garcia-Gracia, R. El-Ganainy, D. N. Christodoulides, and M. Khajavikhan, Enhanced sensitivity at higher-order exceptional points, Nature **548**, 187 (2017).
[73] S. Wang, B. Hou, W. Lu, Y. Chen, Z. Q. Zhang, and C. T. Chan, Arbitrary order exceptional point induced by photonic spin-orbit interaction in coupled resonators, Nat. Commun. **10**, 832 (2019).